Cellular/Molecular

Extracellular Potentials Modify the Transfer of Information at Photoreceptor Output Synapses in the Blowfly Compound Eye

Matti Weckström[1,2] and Simon Laughlin[3]

[1]Department of Physics, Division of Biophysics, and [2]Biocenter Oulu, University of Oulu, 90014 Oulu, Finland, and [3]Department of Zoology, University of Cambridge, Cambridge CB2 3EJ, United Kingdom

Signal processing in fly photoreceptors and visual interneurons takes place with graded potentials. Photoreceptors drive large monopolar cells (LMCs) with synapses that, like their counterparts in vertebrates, have a high gain and introduce strong spatiotemporal antagonism (Laughlin et al., 1987) that implements predictive coding (Srinivasan et al., 1982). The synapses are contained in compartments, lamina cartridges, whose extracellular potentials change with illumination (Shaw, 1984). We described these extracellular field potentials (FPs) using a novel permeabilization technique that converts neurons into extracellular recording probes. Having characterized extracellular FPs, we went on to study them using conventional microelectrodes. Extracellular space in a cartridge is electrically isolated from the body cavity and retina [input resistance (R_{in}) = 6.0 MΩ in dark], and light adaptation increases this isolation (R_{in} = 7.8 MΩ). In the dark, the extracellular space is 30 mV hyperpolarized compared with retina, and this promotes tonic synaptic activity by depolarizing the synaptic terminals. Illumination depolarizes the extracellular space, and voltage-clamp studies suggest that the postsynaptic chloride current in LMCs contributes to this light response. The presynaptic transmembrane potential in the photoreceptor axon was estimated by subtracting the FP from intracellular recordings. By backing off the presynaptic input, the FP can reset the synaptic operating range, produce response transients, and contribute to predictive coding by subtracting redundant low frequencies.

Introduction

Neurons can communicate by polarizing the extracellular space around voltage-gated ion channels (Faber and Korn, 1983; Jefferys, 1995). There are strong indications that local polarization of the extracellular space around photoreceptor synapses is used to subtract redundant signal components. Fish retinal horizontal cells have hemichannels, apparently capable of injecting current into the extracellular space of the cone pedicle to produce lateral inhibition and chromatic opponency in bipolar cells (Byzov and Trifonov, 1968; Byzov and Shura-Bura, 1986; Kamermans et al., 2001). Insect compound eyes exhibit large extracellular field potentials (FPs) (Mote, 1970) associated with resistance barriers surrounding photoreceptor axon terminals (Shaw, 1975, 1984), which could subtract redundant components by changing the presynaptic membrane potential (Laughlin, 1974, 1981; Shaw, 1978, 1984; Zimmerman, 1978) (see Fig. 1, schematic descriptions). Presynaptic subtraction is supported by measurements of presynaptic calcium currents (VanLeeuwen et al., 2009) and postsynaptic conductance (Laughlin and Osorio, 1989; Weckström et al., 1989; Kamermans et al., 2001).

Received Dec. 9, 2009; revised May 20, 2010; accepted May 30, 2010.

This work was supported by grants from the Academy of Finland and from the Sigrid Juselius Foundation. We are also grateful to Paivi Kettunen for her contributions in the earlier stages of this work, and to Mikko Vähäsöyrinki for constructive comments.

Correspondence should be addressed to Matti Weckström, Department of Physics, Division of Biophysics, and Biocenter Oulu, University of Oulu, 90014 Oulu, Finland. E-mail: matti.weckstrom@oulu.fi.

DOI:10.1523/JNEUROSCI.6122-09.2010

 0270-6474/10/309557-10$15.00/0

The advantage of investigating the action of extracellular potentials on photoreceptor synapses in blowfly compound eye is that they are generated in a well defined structure: the lamina cartridge (Shaw, 1984). A cartridge is a glial-bound cylinder that contains the axon terminals and output synapses of six achromatic photoreceptors (designated R1–6). These six photoreceptors code a single image pixel because their axons project from the retina to the lamina according to the neural superposition principle (Kirschfeld, 1967). Within the cartridge (see Fig. 1*A*), the six photoreceptor axon terminals synapse onto the three large monopolar cells (LMCs), L1, L2, and L3 (Fröhlich and Meinertzhagen, 1983) at ~1200 tetrads. The postsynaptic responses of blowfly LMCs are well documented (Autrum et al., 1970; Zettler and Järvilehto, 1971; Laughlin and Hardie, 1978; Juusola et al., 1995a) (for review, see Laughlin, 1994; Juusola et al., 1996) because they are amenable to high-quality intracellular recordings in intact preparations. Despite these advantages, the ability of the extracellular field potential within a cartridge to regulate synaptic transmission is uncertain. Putative recordings of field potentials vary considerably in amplitude, and their responses to light are often contaminated with signals from damaged cells (Laughlin, 1974). Consequently, neither the magnitude of the field potential nor the waveform of its light responses has been established. There could also be subcompartments within the cartridge.

Here, we offer a new solution to the problem of recording FPs from extracellular space. By inserting an intracellular micropipette into a neuron and permeabilizing its membrane, we convert this neuron into an extracellular recording probe that samples the

FP in the immediate surroundings of the cell. By permeabilizing LMCs, we obtain consistent recordings that identify an FP within a lamina cartridge, and in subsequent experiments we search for and record such FPs using micropipettes filled with potassium acetate. This eliminates permeabilization artifacts and allows us to estimate the ability of extracellular potentials to regulate synaptic transmission. We find that FPs can contribute to retinal coding by subtracting DC and low-frequency signal components from photoreceptor outputs. We suggest that extracellular potentials are used to regulate photoreceptor output synapses because they are economical, integrate population signals, and are relatively noise free.

Materials and Methods

Our approach was to first identify the FP in the lamina cartridge using intracellular recordings from LMCs that were permeabilized to connect them to extracellular space. Thereafter, we used conventional potassium acetate-filled electrodes for the longer term recordings that were needed to investigate FPs more thoroughly. The use of potassium acetate electrodes excludes the possibility of artifacts produced by the permeabilizing agent leaking into the cartridge and damaging other neurons and glia. We still do not know how many electrical compartments are contained within a lamina cartridge, but with permeabilization it is possible to record from extracellular space that is immediately adjacent to an identified LMC.

The recordings. Recordings were made from the retina and lamina of intact restrained blowflies, *Calliphora vicina*, using single-electrode current-clamp and single-electrode voltage-clamp techniques (Finkel and Redman, 1984) that have been successfully applied to the small neurons of the blowfly retina (Laughlin and Osorio, 1989; Weckström et al., 1989, 1991, 1992b; Hardie and Weckström, 1990). Glass capillary electrodes (Clark Electromedical) were pulled with a P-80 PC (Sutter Instruments). They were advanced with a piezoelectric micromanipulator (PZ-550, Burleigh) through a small hole in the head capsule behind the eye, which was sealed with silicon high-vacuum grease. The electrodes were filled with 2 M K-acetate and 4 mM KCl, and buffered to pH 6.50 with K-phosphate saline to facilitate current passing. For intracellular recordings, the electrode resistances were in the range 70–170 MΩ. The majority of extracellular field potentials were recorded with relatively blunt electrodes ($R_e < 60$ MΩ) to reduce the possibility of contamination of the extracellular response by signals generated within damaged cells. An indifferent thin Ag–AgCl electrode was inserted to a depth <0.5 mm into either the base of the ipsilateral retina or the thorax hemolymph and attached to the other input of the high-impedance switched clamp preamplifier (SEC-I L, NPI Electronic). In the single-electrode voltage clamp, the switching frequency was set between 2.5 and 5 kHz. The time constant of the electrodes (with capacity compensation) was <5 μs, and that of membranes of clamped LMCs was 0.5–1 ms, and was therefore in accordance with the rules for single-electrode clamping (Weckström et al., 1992b). Signals were recorded and analyzed on a PC using custom-made programs.

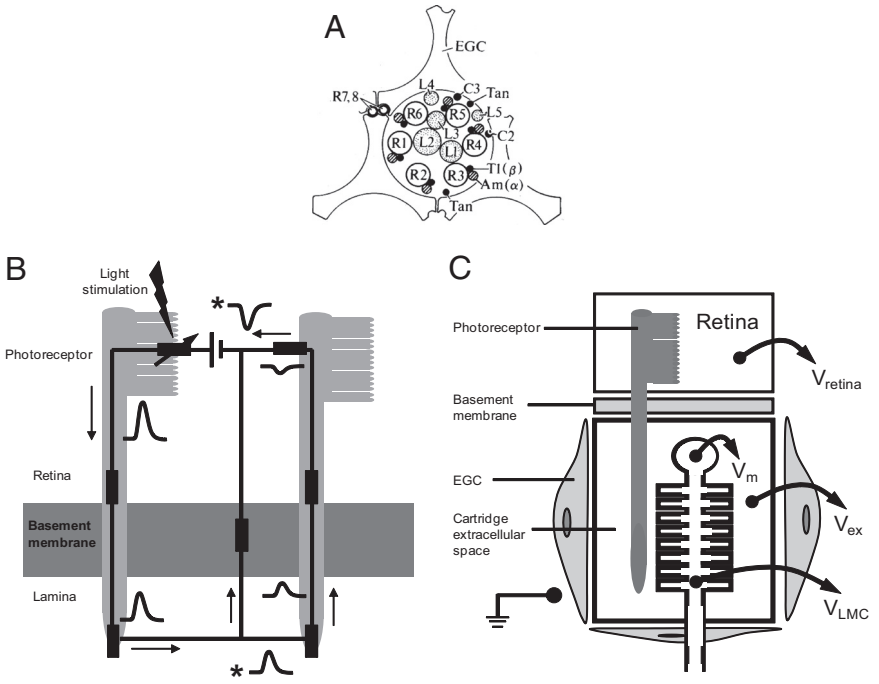

Figure 1. Schematics showing the basic cellular and electrical structure of a lamina cartridge in the first optic neuropile of the fly. ***A***, Transverse section through the synaptic zone of a cartridge showing the positions of the major cellular elements (redrawn after Shaw, 1981). The ring of axon terminals of the six achromatic photoreceptors coding the same image pixel (R1–R6) form ~1300 tetradic output synapses, within which the three LMCs L1, L2, and L3 act as postsynaptic elements. The smaller elements are the two chromatic photoreceptors R7 and R8, the interneurons L4, L5, T1, and C2, and the lamina amacrine cells Am(α). Three epithelial glial cells (EGC) form a sheath around the cartridge that encloses the extracellular space and restricts diffusion between neighboring cartridges (redrawn after Shaw, 1981, 1984). ***B***, Basic electrical circuit showing how current leaving photoreceptor terminals depolarizes the extracellular space in a lamina cartridge (redrawn after Shaw, 1975). The left-hand side of the circuit shows light-gated current entering the photoreceptor soma in the retina and leaving via its axon terminal in the lamina. To complete the circuit, the current passes from lamina extracellular space back to retina and, by crossing a glial resistance barrier at the basement membrane, depolarizes the lamina extracellular space. This depolarization can also drive return current through neighboring, less-stimulated photoreceptors (right-hand side). The waveforms indicate voltage responses to a flash of light at different locations in the circuit, all of which are measured relative to a reference electrode in the hemolymph. Responses recorded from extracellular space are denoted by an asterisk. The rest represent intracellular recordings. ***C***, A schematic of the projection of a photoreceptor from the retina to a postsynaptic LMC in a lamina cartridge. The photoreceptor axon penetrates the resistance barrier at the basement membrane and enters the cartridge, which is a compartment bounded by EGCs. The extracellular potential within this compartment, V_{ex}, biases the membrane potentials of cells within it. As shown for an LMC, the transmembrane potential V_m is the intracellular potential V_{LMC}, recorded relative to a common reference minus the V_{ex} recorded relative to the same reference. In our experiments, the reference was either the earth shown in the body cavity or, more frequently, the extracellular potential in the retina, V_{retina} (see text for further details).

Light stimuli. The stimulus was a green, 555 nm light-emitting diode (LED), mounted on a Cardan arm that rotated the light source at a constant distance of 45 mm around the eye. The light intensity was controlled with a custom-made, linearized voltage-to-current converter, controlled by the computer digital/analog output. The 555 nm light mainly stimulates the R1–6 photoreceptors (Hardie, 1987). The angular subtense of the LED was 0.8°, which is small compared with the receptive field of the lamina FP (≈45° vertical and >45° horizontal when the eye is dark adapted), or with R1–6 photoreceptors (~1.5°). We can confidently assume that at low light intensities mainly photoreceptors within one neuro-ommatidium were being stimulated, although some stray light necessarily stimulates neighboring ommatidia. LED outputs were measured with a photometer (Opt-O-Meter 80X, United Technology) and were converted to multiples of absorptions of single photons per R1–6 photoreceptor per second. These photon rates were defined by counting the small, discrete depolarizations in photoreceptors evoked by single photons at low light levels (Lillywhite, 1977; Laughlin et al., 1987; Juusola et al., 1994). The purpose of this method was to relate the intensities to the functional range of the photoreceptors, and not to suggest a photon flux that is exactly correct for each photoreceptor. Given that a

number of previous studies have used this measure, it is a more useful way than log-units attenuation of the source for presenting light intensity. The stimulus protocols included brief flashes, pulses, and step increments to new steady background levels, and increments and decrements about a steady background. Sequences of band-limited, pseudorandomly modulated noise stimuli were used to obtain frequency responses (Juusola et al., 1994). The power spectra of voltage responses to this stimulus were calculated via the fast Fourier transform by standard methods, including time domain and ensemble averaging (Bendat and Piersol, 1971; Kouvalainen et al., 1994) using a Blackman–Harris four-term window (Harris, 1978).

Membrane permeabilization with the DMSO. To record the extracellular voltage responses generated in the immediate surroundings of a photoreceptor or an LMC (Fig. 1*C*, V_{ex}), the cell was impaled with an intracellular electrode (yielding recordings of V_{LMC}) (Fig. 1*C*). Its membrane was then permeabilized by injecting iontophoretically a detergent, 2.5 mM DMSO (Sigma) that had been added to the electrode filling solution (2 M K-acetate and 5 mM KCl). The injecting current was −0.25 to −1.0 nA, delivered either continuously or with a 30–50% duty cycle. The time taken to permeabilize a cell varied from ~5 to 25 min. The two recorded voltages (V_{ex} and V_{LMC}) could then be subtracted to obtain an estimate of V_m, supposing that these two voltages are in series, as shown in Figure 1*C*.

Cell identification and response criteria. R1–6 photoreceptors and postsynaptic LMC neurons, L1–3, recorded in retina and lamina could be reliably identified by functional criteria (Weckström et al., 1992a; Uusitalo et al., 1995b). The other types of cells found in the lamina cartridge were not encountered in our recordings, but we presume they were stimulated. These would have included epithelial glial cells in the lamina, which are postsynaptic elements at a sizeable fraction of the R1–6 axon tetrads (Shaw, 1984). This strong synaptic drive to glia has some bearing on the interpretation of the results.

To exclude poor impalements, the photoreceptor and LMC responses had to satisfy the following criteria, which are based on our previous work with these cells (Hardie and Weckström, 1990; Weckström et al., 1991, 1992a). The dark resting potential had to be more negative than −55 mV for photoreceptor somata and axons, −30 mV for L1 and L2, and −55 mV for L3. The saturated voltage response to light had to exceed 50 mV in photoreceptor somata, 30 mV in photoreceptor axons, and 20 mV in LMCs. Input resistance had to be >25 MΩ for photoreceptor somata, >50 MΩ for photoreceptor axons, >10 MΩ for the L1 and L2, and >20 MΩ for L3. LMCs with responses that depolarized above the dark resting level during a prolonged illumination were excluded because this indicates a damaged cell that is picking up the FP. The criteria for identifying the FP when recording with conventional potassium acetate-filled electrodes were established by recording from permeabilized cells and are described in more detail in the Results. In the lamina, the FP in the dark had to be between −30 and −20 mV, there had to be an ~5 MΩ resistance to the indifferent electrode, and the characteristically slow and noiseless waveform of the response to light stimulation had to have an amplitude >20 mV.

Recordings were made from 23 photoreceptor somata in the retina, and 32 photoreceptor axons and 53 LMCs in the lamina. There were 57 recordings of FPs in lamina cartridges.

Results

Experimental approach

We set out to see how the FP in the extracellular space of a lamina cartridge can modify the presynaptic membrane potential at the photoreceptor output synapse. FPs are set up across extracellular resistance barriers, as depicted in Figure 1. Tracer experiments (Shaw, 1984) have established that an extracellular resistance barrier separates the retina and the lamina from each other and from the hemolymph of the body cavity (Fig. 1*B*,*C*). Each is, therefore, a distinct compartment, capable of sustaining its own FP. The lamina is further subdivided into cartridges by epithelial glial cells, which also impede diffusion (Shaw, 1984). Thus, the presynaptic membrane potential at the photoreceptor synapses is

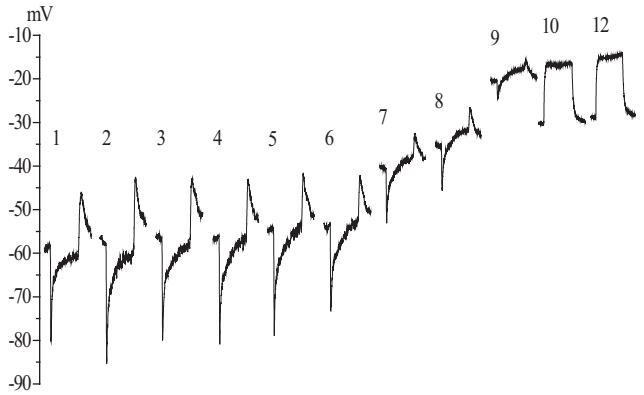

Figure 2. The effect of DMSO injection on the membrane potential recorded from a dark-adapted LMC. After penetration by a DMSO-filled micropipette, the dark resting membrane potential of the LMC and its response to a 300 ms light step (10^6 photons/s) were measured at 1 min intervals. This series of responses is plotted as a series with the time after penetration in minutes above each response. Each response waveform is the average of three responses delivered 0.5 s apart and is positioned with its initial baseline at the prevailing dark resting potential. DMSO injections were started after measuring the response at 1 min, and they were performed by means of −0.25 nA current pulses lasting 300 ms, repeated with 1 s intervals. The original dark resting potential of the cell was −55 mV. During the first 5 min the on-response reduced from 40 to 30 mV without a significant change in the dark resting potential. After this, the dark resting potential depolarized by 20 mV, and a clear depolarizing plateau appeared in the response. After 10 min, the hyperpolarizing response of the LMC disappeared, leaving just the depolarizing response. The reason for the reduction of the dark resting potential in this recording between the 9th and 10th minutes was not clear, but this was not a common feature in the DMSO experiments. The final dark resting potential, indicative of the lamina extracellular space, was −32 mV.

defined as the intracellular potential recorded from within the photoreceptor axon relative to a reference potential, minus the FP in the extracellular space adjacent to the synapse, when recorded relative to the same reference potential (Fig. 1*B*,*C*). The same argument applies to the membrane potential of the postsynaptic LMC, within the cartridge.

In some of our experiments, the reference potential was measured with a relatively large electrode (Materials and Methods) implanted in the extracellular hemolymph of the thorax. This allows us to measure the intracellular potentials of axons and LMCs, and the extracellular potentials of the retina compartment and lamina cartridge compartment relative to body cavity (Fig. 1*C*, the earth). However, we generally preferred to insert the large reference electrode into the ipsilateral retina at the base of the eye because the recordings were more stable and were not perturbed by muscle potentials. The electrode at the base of the eye did not pick up the change in extracellular potential recorded close to stimulated photoreceptors (the focal ERG, see below) because we only stimulated photoreceptors in the upper half of the eye. Consequently, the potential recorded at the base was, for all practical purposes, equal to the ground in the body cavity.

We faced the problem encountered by many previous investigators. Potentials recorded with blunt electrodes placed in the lamina, supposedly recording only the extracellular signal, vary considerably in amplitude and waveform, presumably according to the exact location of the electrode tip (Laughlin, 1974). This is despite the fact that the lamina cartridge is a well defined structure bounded by extracellular resistance barriers (Shaw, 1984) (Fig. 1). These variations could have resulted from partial neuron impalements, interference from glia, and the insertion of the electrode into different subcompartments of the lamina extracellular space. To obtain reliable measures of the electrical potential of the

extracellular space surrounding the photoreceptor–LMC synapses in the lamina cartridge, we devised the permeabilization technique (see Materials and Methods). Permeabilization, by intracellular injection of the detergent DMSO, converts an LMC or a photoreceptor axon terminal into a recording probe, situated in the extracellular space of the synaptic zone of the lamina cartridge. This effect of permeabilization can be seen in Figure 2. During a 10 min injection of DMSO into an LMC, the hyperpolarizing response of this neuron to light stimulation was reduced, and it was eventually replaced by a depolarization. At the same time, the resting potential progressively moved upward to a stable, less hyperpolarized value. In this particular recording, the value went from −55 to −32 mV.

Having established the properties of the lamina extracellular FP by recording from 28 permeabilized LMCs, we then switched to using electrodes filled with potassium acetate. With these conventional electrodes, we could locate, record, and study the FP intensively without being concerned that the detergent DMSO was causing artifacts by leaking into neighboring cells. The extracellular recordings made with DMSO electrodes and with conventional K-acetate-filled electrodes were stable for minutes to tens of minutes.

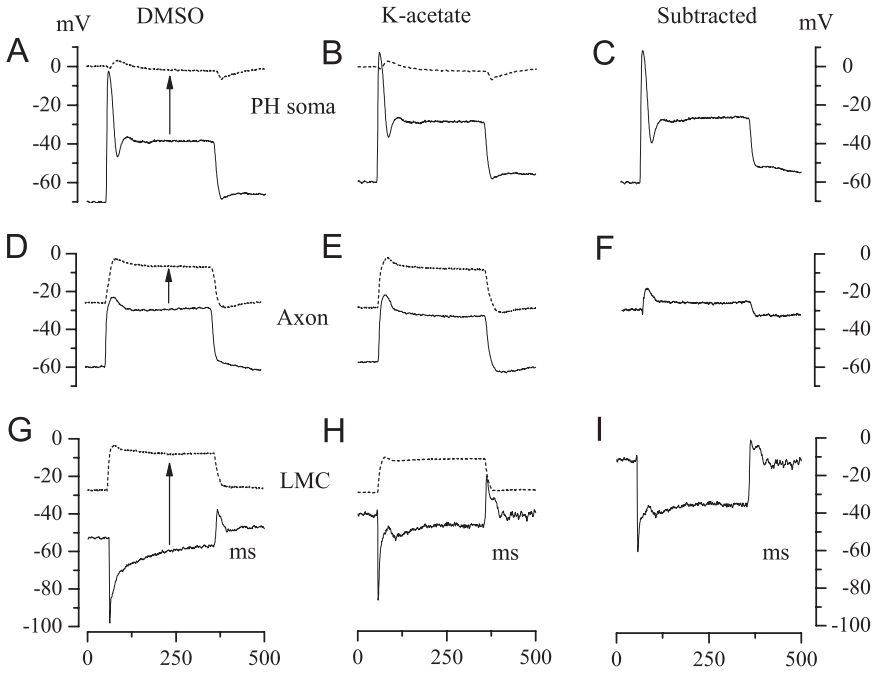

Figure 3. A summary of our experimental approach to recording the FP from extracellular space and determining its effect on the transmembrane potentials of photoreceptors and LMCs. ***A***, ***B***, ***D***, ***E***, ***G***, ***H***, The solid traces show intracellular recordings from a photoreceptor soma in the retina (***A***, ***B***), and from a photoreceptor axon (***D***, ***E***) and an LMC (***G***, ***H***) in lamina cartridges. Membrane potentials were recorded relative to a common reference. Light responses were evoked by 300 ms pulses of 10^6 photons/s delivered at 1 s intervals. Two approaches were used to determine the extracellular FP (dashed traces) at the sites of these intracellular recordings. Cells were penetrated with electrodes containing DMSO (left-hand column), identified from properties recorded immediately after penetration (e.g., solid traces), and then permeabilized with DMSO to record the FP (dashed traces). In the second approach (middle column), a micropipette filled with K-acetate was used to record intracellularly from an axon or an LMC in a cartridge, and then repositioned to record from extracellular space close to the site of the intracellular recording. ***C***, ***F***, ***I***, Subtraction of the extracellular record from the intracellular record gives the transmembrane potential (right column). Each trace is the average of three responses.

Figure 3 provides an overview of the results obtained by applying this approach. The left column of Figure 3 shows light responses recorded with permeabilizing (DMSO) electrodes from a photoreceptor soma in the retina (A), a photoreceptor axon in a lamina cartridge (D), and an LMC in a lamina cartridge (G). At the beginning of an experiment, immediately after impalement and before permeabilization, one sees the normal robust intracellular response to a bright light pulse (continuous lines). After permeabilization, one sees the FP in the immediate vicinity of the impaled cell (dotted lines). The arrows indicate the shift from the intracellular to the extracellular potential. The middle column compares FPs (dotted lines) and intracellular responses recorded with conventional potassium acetate electrodes (continuous lines). The right column of Figure 3 shows estimates of the transmembrane potential (Fig. 1*C*, V_m) obtained by subtracting the FP from the intracellular response.

Proving the permeabilization technique on photoreceptors

To observe the time course of permeabilization and confirm that it produces a true estimate of the extracellular potential, we first applied the technique to photoreceptor somata in the retina. If the method works, permeabilization should result in a depolarization to zero voltage, i.e., equal to the reference electrode located in the retinal extracellular space at the base of the eye. Permeabilization by the iontophoretic injection of DMSO progressed more slowly in photoreceptors (>40 min) than in LMCs (e.g., 10 min) (Fig. 2). As expected, the advance of permeabilization was accompanied by a diminution of light response, a steady depolarization from an initial resting potential of approximately −55 mV to zero relative to the reference in the retinal extracellular space, and a reduction of input resistance from >25 MΩ to 1–2 MΩ. This residual resistance suggests that a low resistance barrier exists between the retina and the hemolymph. Photoreceptor permeabilization was completed in 40–50 min and produced a light response (Fig. 3*A*, dotted trace) identical to those obtained with conventional (potassium acetate) electrodes inserted in the extracellular space of the retina (Fig. 3*B*, dotted trace) and consistent with the normal focal ERG recorded close to stimulated ommatidia with relatively sharp electrodes. The focal extracellular response to a light step had a biphasic onset, and a small depolarization followed by a slow hyperpolarization that peaked 25–30 ms after the stimulus was turned off at a value of −6.5 ± 1.9 mV (mean ± SD, n = 17/6, DMSO/K-acetate, respectively).

Permeabilization of axon terminals and LMCs

Photoreceptor axon terminals and LMCs were impaled in the lamina (Fig. 1) and permeabilized by injecting DMSO to identify and measure the extracellular potential inside lamina cartridges. Immediately after penetration, the responses of photoreceptor axons and LMCs to 300 ms light pulses were normal (Fig. 3*D*,*G*, continuous traces); i.e., their amplitudes and waveforms were consistent with earlier reports (Weckström et al., 1992a). Cells were then permeabilized, as in the photoreceptor somata recordings, to record the FPs in their immediate vicinities (Fig. 3*D*,*G*, dotted traces). Because the effect of DMSO on LMCs took ~5–25 min to develop (Fig. 2), we had time to identify the interneuron type (L1, L2, or L3) according to the light response, the dark

resting potential, and also the input resistance with a small hyperpolarizing pulse of current injection (Hardie and Weckström, 1990; Uusitalo et al., 1995b) (see Materials and Methods for criteria). The FPs recorded from all four types of permeabilized cells (axon terminal, L1, L2, and L3) were essentially identical, despite the fact that these cells occupy different positions within the cartridge (Fig. 1*A*).

On the basis of 31 recordings from permeabilized cells, 3 from axons and 28 from LMCs, we established the following criteria for recordings of FPs from intracartridge extracellular space. In the dark, the potential of the extracellular space was approximately −20 to −30 mV. Light pulses induced a graded depolarization that increased in amplitude with intensity to ~20 mV at the highest available light levels (Figs. 2, 3). This depolarization contained less noise than intracellular recordings from photoreceptors. The variance of the voltage responses during a 100 ms stimulation at 10^5 photons/s was ~0.1 mV^2 in photoreceptor axon recordings, while it was ~0.02 mV^2 in FP responses ($n = 4$). At higher light levels, the FP recordings had small, rounded transients at stimulus onset. The resistance recorded between the electrode in intracartridge extracellular space and the indifferent electrode in the retinal extracellular space (for structural considerations, see Fig. 1) was relatively low, on the order of 5 MΩ in the dark.

Measuring the FP with potassium acetate electrodes

The criteria established with permeabilized cells enabled us to tell when potassium acetate electrodes were recording FPs reliably from the extracellular space within a cartridge. We could then carry out longer experiments with these conventional electrodes without the risk that the permeabilizing detergent would disrupt the lamina cartridge. In these conventional recordings, the potential difference in the dark between the extracellular space in the retina and the extracellular space within the lamina cartridge was −27.6 ± 3.5 mV ($n = 21$). This value did not depend on the direction in which the electrode approached the lamina (i.e., from retina or directly into the lamina via the back of the head capsule) and is within the range of previously published reports (Mote, 1970; Laughlin, 1974; Shaw, 1975).

The FP helps to determine the membrane potentials of cells within the lamina cartridge. Relative to the retinal extracellular space, and hence the hemolymph of the body cavity, the dark resting potential of photoreceptor axon terminals was −60.3 ± 3.9 mV ($n = 32$), for LMCs L1 and L2 it was −41.6 ± 8.1 mV ($n = 18$), and in the putative L3s it was −59 ± 8.4 mV ($n = 7$). These values are in good agreement with previous reports (Uusitalo and Weckström, 1995b). Subtracting the average extracellular dark potential, −27.6 mV, gave estimates of true transmembrane potentials in darkness of −33 mV in the photoreceptor axons, −14 mV in the LMCs L1 and L2, and −31 mV in the LMC L3. The effects of subtracting FPs from recordings of light responses are shown in the right-hand column of Figure 3, *C*, *F*, and *I*, for a photoreceptor soma in retina, a photoreceptor axon in lamina, and an LMC in lamina, respectively. This example shows that the FP has a major impact on the light-induced changes in the transmembrane potentials of axons and LMCs in the lamina; axon responses are smaller and more transient (Fig. 3*F*), while LMCs exhibit a larger sustained response after the initial on-transient (Fig. 3*I*).

Given the pronounced effects of the FP on neuronal light responses, the response of the FP to light was described in more detail. When dark adapted, the maximum amplitude of the FP response to a brief flash (Fig. 4*A*, left) was 15 ± 4.1 mV ($n = 10$).

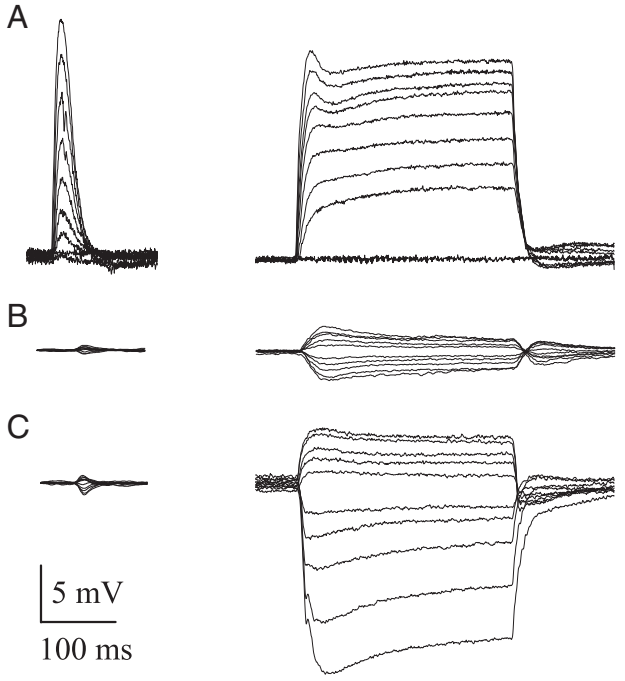

Figure 4. The light responses of FPs recorded from lamina cartridges under different conditions of illumination. ***A***, Dark-adapted conditions; responses to a 2 ms flash (left) or a 300 ms pulse (right), increasing progressively in intensity from 500 photons/s (lowest amplitude response) to 10^6 photons/s (highest amplitude response). ***B***, Light-adapted responses to a background level of 10^3 photons/s. Responses to 2 ms flashes and 300 ms pulses with contrasts increasing in 0.2 increments from −1 to +1. ***C***, Light-adapted responses to a background level of 10^6 photons/s, pulse duration, and contrast as in ***B***.

Longer light pulses (300 ms) evoked depolarizations of 23 ± 3.8 mV ($n = 21$) (Fig. 4*A*, right). The FP response had a characteristically slow rise time. The step response to small-intensity light pulses rose monotonically according to a first-order exponential ($\tau = 30 \pm 20.1$ ms; $n = 7$). However, with higher intensity pulses the response was faster and its shape more complicated. FP responses were recorded and examined at several background light levels (Fig. 4*B*,*C*). At low background light levels (10^3 photons/s), the responses to increments and decrements around the adapting light intensity varied approximately linearly with stimulus contrast (Fig. 4*B*). At high-intensity backgrounds (e.g., 10^6 photons/s) (Fig. 4*C*), the steady-state depolarization was 10–15 mV, and negative contrast steps elicited larger responses than positive ones (Fig. 4*C*). With a background of 10^6 photons/s, a response of −1.7 ± 2.0 mV was evoked by a 2 ms pulse of contrast of −1.0, compared with +0.70 ± 0.84 mV response to a pulse of contrast of +1.0 (Fig. 4*C*, left). The corresponding values for 300 ms steps were −13 ± 1.0 and +4.7 ± 0.84 mV (Fig. 4*C*, right). The FP retained a relatively slow and relatively noise-free waveform at all background light levels.

The synaptic zone is electrically isolated from the hemolymph

As originally demonstrated by Shaw (1975) in the locust eye, electrical isolation of the extracellular space of the first optic neuropile (the lamina) is a prerequisite for a large FP. The degree of isolation was measured by injecting small current pulses (−0.2 nA, 300 ms) into the extracellular space, via the recording electrode, and measuring the resultant polarization. This is shown in Figure 5 for locations in retina (Fig. 5*A*) and lamina (Fig. 5*B*). Dividing the polarization at the end of the current pulse by the current amplitude gives the extracellular input resistance (R_{in})

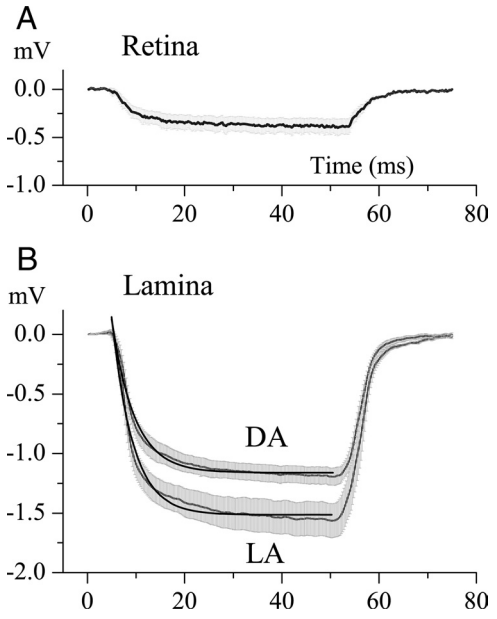

Figure 5. The change in potential produced by injecting current into the extracellular space of the retina and the lamina. ***A***, Polarization of the retinal extracellular space by a −0.25 nA current pulse lasting 50 ms. The charging curve has a time constant ≈5.0 ms, and the amplitude of response at the end of the pulse indicates a resistance of 1.9 MΩ. Data were averaged over five experiments; range bars show the SE. ***B***, Polarization of the lamina intracartridge space under dark-adapted (DA) and light-adapted (LA) conditions. Data obtained are as in ***A*** and were averaged for >10 experiments for DA and 6 experiments for LA conditions. Range bars show the SE. The dark thick lines are first-order exponentials that indicate time constants of 4.0 ms for DA conditions, and 4.2 ms for LA conditions. Assuming a simple RC circuit model for the extracellular compartment, this yields resistances of 6.0 ± 0.45 MΩ for DA conditions and 7.8 ± 0.78 MΩ for LA conditions, and apparent capacitances of 0.71 nF (DA) and 0.51 nF (LA).

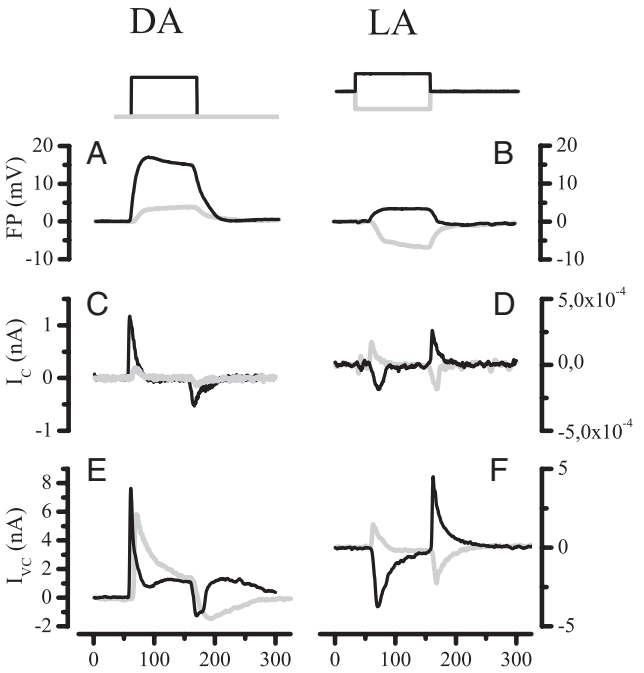

Figure 6. A comparison between the properties of the FP and the voltage-clamped current in LMCs, I_C, measured under dark-adapted (DA) and light-adapted (LA) conditions. The top traces show the step stimuli: DA, 10^2 photons/s (gray), and 10^6 photons/s (black); LA, contrasts ±1.0 (positive, black; negative, gray) applied against a background of 10^6 photons/s. ***A***, Dark-adapted FP responses to large (black) and small (gray) step stimuli. ***B***, Light-adapted FP responses to positive (black) and negative (gray) contrasts. ***C***, ***D***, The first derivatives (dV/dt) of the FP; trace color (black or gray) indicates stimulus as above. These plots indicate the time courses of the currents required to create the corresponding FPs, were they membrane potentials. Note that the currents are plotted in arbitrary units. ***E***, ***F***, Voltage-clamp currents recorded from LMCs under the same conditions as the FPs; trace colors (black or gray) are indicated as above. LMCs were clamped at the dark resting potential. Note the similarity between the dV/dt curves (***C***, ***D***) and the LMC currents.

with respect to the indifferent electrode. In the retina (Fig. 5*A*), the extracellular R_{in} to an indifferent electrode in the hemolymph was 1.5 ± 0.79 MΩ ($n = 5$) regardless of the mean illumination level. This result shows that any barrier separating the retina from the hemolymph must be small. Interestingly, measurements made using an indifferent electrode situated at the base of the ipsilateral eye gave a similar result, and this suggests that the resistance is located in the retina, between the focal recording site at the top of eye and the indifferent electrode at the base.

Cartridges within the first optic neuropile, the lamina, were considerably more isolated from both the retina and the hemolymph, and the degree of isolation increased with light adaptation (Fig. 5*B*). For the extracellular space within a cartridge, R_{in} was 6.0 ± 0.45 MΩ ($n = 10$) under dark-adapted and 7.8 ± 0.78 MΩ ($n = 6$) under light-adapted conditions (10^6 photons/s). The difference, as measured with *t* test, is also statistically significant ($t = 7302$, $p < 0.001$). The charging curves did not strictly follow first-order (simple RC, a circuit with a resistor and a capacitor in parallel) kinetics. Nonetheless, we defined the first-order time constants by curve fitting to obtain a rough approximation of the electrical properties of the intracartridge space. The time constants were 4.2 ms in the dark-adapted and 4.0 ms in the light-adapted conditions. The corresponding estimates of capacitances derived from these measurements (dividing obtained time constants by average values of the R_{in}) were 0.71 and 0.51 nF.

FP generation

We cannot readily identify the processes responsible for the dark (steady-state) hyperpolarization of the lamina extracellular space at present. However, we can deduce the current required to reduce the level of hyperpolarization during illumination. The simplest hypothesis is that the time course of this reduction, in other words the time course of the response to light of the FP, is directly proportional to fast neuronal transmembrane currents that flow into or out of the extracellular compartment. The forms of those currents can be estimated by taking the first time derivative of the extracellular voltage signal, $FP(t)/dt$, based on the assumption that the voltage is a result of membrane charging, whatever the membrane. The estimate was made for exemplary field potentials recorded in two conditions, dark adapted (Fig. 6*A*) and light adapted (Fig. 6*B*). The currents predicted by this procedure (Fig. 6*C*,*D*) are strikingly similar in time course to synaptic currents in LMCs, recorded with single-electrode voltage clamp *in situ*, under equivalent conditions (Fig. 6*E*,*F*), although there are also some differences. LMC responses are dominated by the histamine-gated chloride conductance of photoreceptor output synapses (Hardie, 1989; Laughlin and Osorio, 1989; Zettler and Straka, 1987), suggesting that this synaptic chloride conductance, or fast mechanisms that are tightly coupled to it, make a significant contribution to the FP.

The ability of the FP to determine synaptic transmission

Light pulses stimulate a rapid depolarization of the presynaptic terminal of a photoreceptor that, by releasing histamine, causes a rapid hyperpolarization of the postsynaptic LMC (for review, see Laughlin, 1994; Juusola et al., 1996). The light-induced depolarization of the photoreceptor terminal is accompanied by a light-

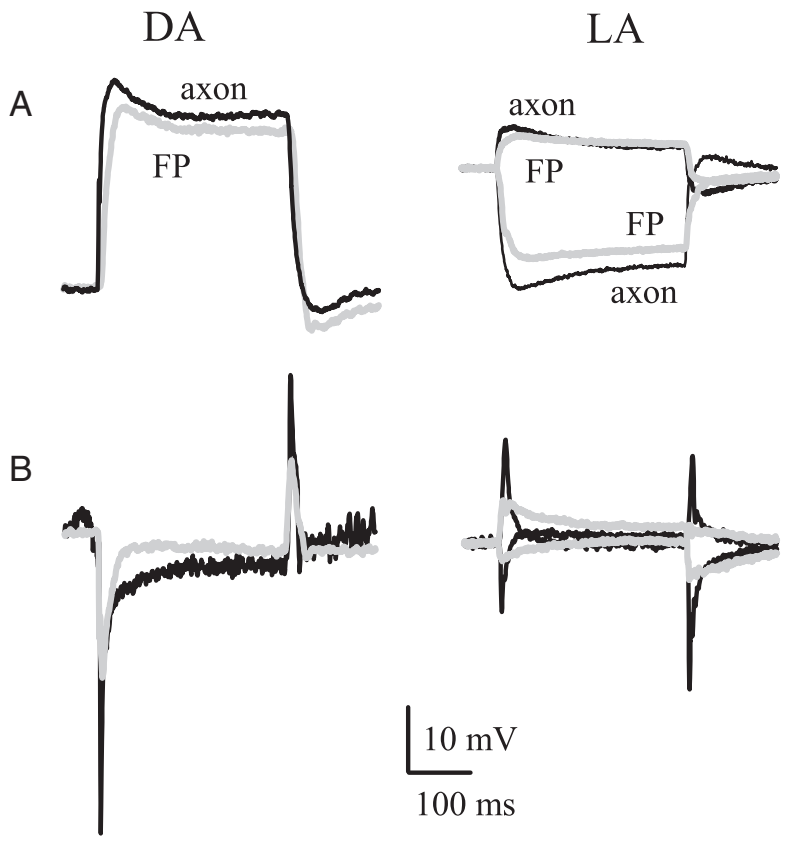

Figure 7. The waveforms of the light responses of FPs, photoreceptor axon terminals, and LMCs under dark-adapted (DA) and light-adapted (LA) conditions. ***A***, FP (gray) and axon (black) responses compared by equating their baselines, just before the stimulus. ***B***, Postsynaptic LMC responses (black traces) compared with photoreceptor axon transmembrane responses (gray traces) calculated from the data in ***A*** by subtracting the FP response from the axon response. The transmembrane potential traces have been inverted for comparison with LMC because the photoreceptor axon–LMC synapses are sign inverting. Note that subtraction of the FP has produced a transient presynaptic signal in the axon that is capable of contributing to the transient postsynaptic response of the LMC. Stimuli: DA, 300 ms light pulse of 10^6 photons/s; LA, 300 ms contrast steps, ± 1 against a background of 10^6 photons/s.

induced depolarization of the FP in the extracellular space around the synapse. As suggested previously (Laughlin, 1974) and illustrated by our recordings (Fig. 3*F*), this extracellular depolarization will oppose the transmission of the photoreceptor signal by reducing the light-induced depolarization of the presynaptic membrane. Thus, the FP is well placed to reduce the redundancy of the transmitted signal (Srinivasan et al., 1982) by presynaptic subtraction (Laughlin, 1974; Shaw, 1975; Laughlin and Hardie, 1978). To assess the contribution of the extracellular FP to the waveform of the postsynaptic response, we recorded the intracellular responses of axons and LMCs and extracellular FPs under identical conditions in the same preparation. We then subtracted the FP from the intracellular responses of the photoreceptor axon to estimate the true time course of the presynaptic membrane potential. These estimates were then compared with the postsynaptic LMC responses (Fig. 7). A 300 ms light pulse delivered to the dark-adapted photoreceptor depolarized the presynaptic terminal by >20 mV (Fig. 7*A*, left, black trace). This depolarization is ~10 mV above the level for synaptic saturation, as measured previously (Laughlin et al., 1987). Subtraction of the FP (Fig. 7*A*, left, red trace) released the synapse from saturation by cutting the presynaptic depolarization back to ~1.5 mV, a value well within the previously measured operating range of the synapse. The difference between the waveform of the presynaptic response and the FP gives an estimate of the presynaptic transient, which was not as sharp in the first few milliseconds as the real postsynaptic response recorded from an LMC (Fig. 7*B*, left side). When the same procedure was performed under light-adapted conditions (Fig. 7*A*,*B*, right side), the subtraction of the field potential again yielded presynaptic transients (Fig. 7*B*, right side, red traces). These transients occurred at the onsets and the offsets of responses to both increments and decrements of light intensity. As in the dark-adapted case, the presynaptic transients generated by subtracting FPs are not as sharp as those actually recorded postsynaptically in LMCs (Fig. 7*B*).

The FP produces transients because it is slower than presynaptic photoreceptor signals. This crucial difference in dynamics was examined by comparing the frequency contents of FPs and photoreceptor signals. The frequency responses were obtained from responses to pseudorandomly modulated light (for details of the methods, see Juusola et al., 1994). The frequency response of the FP was a low-passed version of the photoreceptor response (Fig. 8*A*). Because of the linear property of Fourier transforms, we could calculate the frequency response of the axon terminal by subtracting the frequency responses of the FP from that of the photoreceptor soma. The resulting estimate is shown in Figure 8*B*, along with an earlier estimate of the synaptic transfer function (Juusola et al., 1995a). Although there are likely to be other mechanisms operating in the synapse, it can be seen that our estimate of the presynaptic frequency response shows the same high-pass characteristics as the synaptic transfer function under light-adapted conditions. The high-frequency end is quite different, as expected from earlier studies of LMC responses and the presynaptic photoreceptor terminal (Laughlin et al., 1987; Weckström et al., 1992a; Juusola et al., 1995a,b; Uusitalo et al., 1995b).

Discussion

We have developed a method for measuring extracellular potentials that significantly reduces disruption of the extracellular space by recording electrodes. We impale a cell with a high-resistance microelectrode and then permeabilize the membrane by injecting detergent. Permeabilization converts the neuron into an electrical probe for extracellular space (Figs. 2, 3). We applied the method to photoreceptor axons and second-order neurons (LMCs) in the lamina, the first optic ganglion of the blowfly eye (Fig. 1), and recorded the light-induced changes in extracellular FP (Figs. 3, 4) close to photoreceptor output synapses. Once the properties of the FP were known, subsequent recordings were made with conventional microelectrodes. In the dark, the potential of extracellular space is approximately −30 mV, relative to the body cavity (Figs. 1, 2), and illumination reduces this FP by up to 20 mV (Mote, 1970; Laughlin, 1974; Shaw, 1975, 1981, 1984). By combining our extracellular recordings with intracellular re-

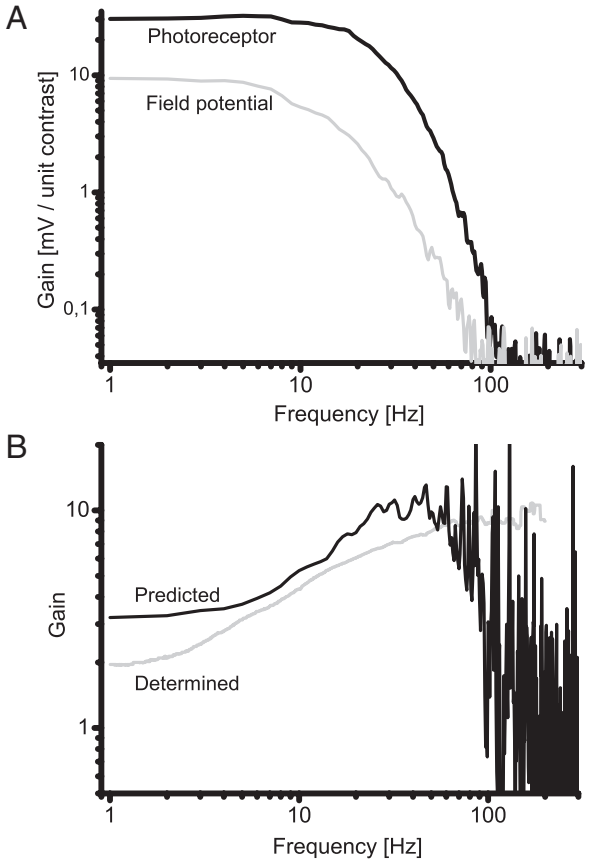

Figure 8. The contribution of the FP to high-pass filtering by the photoreceptor-LMC synapse. ***A***, comparison between the frequency response of a photoreceptor soma recorded in the retina (black) and the field potential (gray) recorded from the extracellular space of a lamina cartridge. Gain, expressed as the millivolt response per unit of stimulus contrast, is plotted versus frequency on logarithmic scales. ***B***, The frequency response predicted for the transmembrane potential of a photoreceptor axon terminal in the lamina cartridge (black) is compared with the frequency response for synaptic transfer from photoreceptor soma to LMC (gray trace) (taken from a previous study by Juusola et al., 1995a). To estimate the frequency response of the transmembrane potential in the photoreceptor axon, we took the data in ***A*** and subtracted the FP response from the photoreceptor response. This procedure suggests that subtraction of the field potential from the presynaptic axon response contributes substantially to the high-pass characteristic of the synapse at frequencies <50 Hz.

cordings from photoreceptor synaptic terminals, we validated previous proposals that the extracellular potential shapes postsynaptic responses (Laughlin, 1974) (Figs. 7, 8). We also estimated the time course of the current required to depolarize the extracellular space (Fig. 6), related it to the postsynaptic responses recorded from LMCs, measured the electrical isolation of the perisynaptic extracellular space (Fig. 5), and discovered that isolation is increased by light adaptation.

Methodological considerations

Because the extracellular space of the neuropile is complex (see Shaw, 1984), sharp electrodes produce variable measures of the extracellular potential, presumably because they partially impale cells (Laughlin, 1974). Permeabilization produces more consistent results. The technique works well in insect lamina because extracellular potentials are generated by several similar cells in a specialized compartment, the cartridge. The technique would fail if a significant part of the FP were generated by current from the permeabilized neuron, or if permeabilization changed the resistance between extracellular compartments. We controlled for these artifacts by comparing neurons that generate responses of opposite polarity and connect different compartments. Photoreceptor terminals depolarize in response to light and connect the lamina to the retina, while LMCs hyperpolarize and connect the lamina to the medulla (Shaw, 1984). When permeabilized, both cell types produced identical results. This can readily be explained because several neurons (three LMCs, six photoreceptor terminals, and several glial cells) can, in principle, contribute to the FP. It may seem surprising that permeabilized photoreceptor axons produced the same FPs as LMCs and are not significantly contaminated by the retinal ERG. However, the resistance of the permeabilized axon terminal is likely to be close to zero, while the resistance of the pathway transmitting current from the retina to the terminal via a thin axon is at least 10 MΩ (the resistance of the photoreceptor soma in the retina under light-adapted conditions). Consequently, any ERG transmitted from the retina to the permeabilized axon terminal will be effectively short circuited to the extracellular space within the cartridge. Finally, artifacts caused by leakage of the detergent (in our case, DMSO) were eliminated by recording identified extracellular potentials with conventional (detergent-free) microelectrodes (Materials and Methods).

Origin of the FP

The mechanisms responsible for generating extracellular potentials around insect photoreceptor output synapses have not been identified. To generate a voltage difference, the charge must cross a resistance barrier (Shaw, 1975). Obvious candidates for this barrier are the glial cells that form tight junctions and isolate the lamina (Shaw, 1984). The increase in the electrical isolation with illumination (Fig. 5) eliminates photoreceptor and LMC axons as candidates, because their resistances decrease with illumination (Laughlin and Osorio, 1989; Weckström et al., 1989, 1991). The extracellular input resistance in darkness, 6 MΩ, is three times the value inferred from models of photoreceptor coupling (van Hateren, 1986). The increase to ~8 MΩ on illumination, and the decrease of apparent capacitance from 0.7 to 0.5 nF, imply decreases in the conductance and effective area of barrier membrane. The numerous photoreceptor synapses onto glial cells suggest a control mechanism (Shaw, 1984), but reliable intracellular recordings from glia are required to confirm this.

What are the ionic currents that hyperpolarize the extracellular space to −30 mV in the dark, and then, in response to light, reduce this hyperpolarization by 20 mV? When using potassium acetate electrodes, the maximum FP light responses were consistently recorded between intracellular recordings from photoreceptor axons with a high input resistance and intracellular recordings from LMCs with the largest on-responses. This correlation implies that the current source is located in the synaptic zone of the cartridge, inside the crown of photoreceptor axon terminals. This location explains why we observed only one type of intracartridge potential even though the cartridge contains at least two extracellular compartments (Shaw, 1984). The consistent amplitudes and waveforms of FPs suggest that the extracellular potential varies little within the synaptic zone and truly represents the presynaptic membrane potential at the site of vesicle release. However, there could be local electrochemical gradients in the extracellular space directly adjacent to release sites shaping synaptic responses, as suggested for pH in mammalian CNS (for review, see Chesler and Kaila, 1992) and vertebrate photoreceptor synapses (Barnes, 1994).

The resemblance between the depolarizing waveform of the FP response to light and the receptor potential (Fig. 3) suggests

that the FP response is generated by current leaving the photoreceptor terminals (Laughlin, 1974; Shaw, 1975). With the measured extracellular resistance of 8 MΩ (Fig. 5), ~2.5 nA is required to generate a 20 mV FP in the light-adapted steady state. However, with resistances of ~100 MΩ (van Hateren, 1986; Weckström et al., 1991; Weckström et al., 1992a), the six photoreceptors axon terminals could only provide ~1.2 nA when depolarized by 20 mV under similar conditions. Other lamina cells must be considered. The similarity between the time courses of the depolarizing current estimated from the rate of change of potential and the synaptically activated chloride current implicates LMCs as sources (Fig. 6). Resistance measurements (Hardie and Weckström, 1990) further suggest that the three large monopolar cells (L1, L2, and L3) could deliver ~1.5 nA. Thus, by acting together, the photoreceptor axons and LMCs could generate sufficient current to depolarize the extracellular space. The origin of the standing hyperpolarization in darkness is not accounted for, but currents maintaining ionic concentration gradients across glial membranes and electrogenic ion pumps in LMCs (Uusitalo and Weckström, 1994; Uusitalo et al., 1995a) could contribute.

Physiological function of the FP

Fly photoreceptor output synapses adaptively filter graded signals (Laughlin et al., 1987; Juusola et al., 1995a, 1996) to optimize coding (Srinivasan et al., 1982; van Hateren, 1992a,b). Our data suggest that polarization of the extracellular space contributes to four aspects of signal processing, namely, the tonic synaptic activity that promotes the high gain, synaptic range shifting, spatial and temporal high-pass filtering, and the intensity-dependent adaptation of high-pass filtering. The high synaptic gain (×10 to ×12) (Laughlin et al., 1987; Juusola et al., 1995a) protects signals from intrinsic noise, and it is achieved by operating the synapse in the steep mid-region of the synaptic characteristic curve (the curve relating output amplitude to input amplitude). Hyperpolarization of the extracellular space depolarizes the presynaptic membrane to −30 mV (Fig. 3*D*,*E*) into the operating range of the L-type Ca^{2+} channels that are thought to sustain transmitter release (for review, see Juusola et al., 1996). The shift in the synaptic characteristic curve by background light is equivalent to voltage subtraction at the presynaptic membrane. Bright backgrounds shift the characteristic curve by >25 mV (Laughlin et al., 1987), and at least 20 mV of this can be accounted for by the field potential. We have probably underestimated this contribution because our point stimulus does not fill the wider receptive field of the field potential (Laughlin, 1974) (M. Weckström, A. Piironen, and S. Laughlin, unpublished observations).

To cope with rapid changes in background light level, the characteristic curve is shifted rapidly, to produce fast transient on- and off-responses in postsynaptic LMCs (Fig. 3). The extracellular potential is not fast enough to form the first few milliseconds of these transients (Fig. 7), but the later decay of postsynaptic response closely follows the shape of extracellular potential. This close correspondence is strong evidence that changes in the extracellular potential are shaping the postsynaptic response by controlling transmitter release, consistent with the transient changes in postsynaptic chloride conductance in LMCs (Laughlin and Osorio, 1989; Weckström et al., 1989). The faster mechanisms have not been identified (Laughlin and Osorio, 1989), but good candidates include both presynaptic and postsynaptic voltage-gated channels (Weckström et al., 1992a; Uusitalo et al., 1995b), feedback mechanisms—e.g., from the amacrine cells (Zheng et al., 2006)—and rapid desensitization of the postsynaptic histamine-gated chloride channels (Skingsley et al., 1995).

Adaptation makes the photoreceptor output synapse into a high-pass filter and, when the retina is fully light adapted, synaptic gain rises linearly with frequency (Laughlin et al., 1987; Juusola et al., 1995a). This filtering optimizes coding by whitening natural signals (van Hateren, 1992b) and the extracellular potential contributes to whitening at frequencies below ~40 Hz (Fig. 8*B*, continuous trace). At lower light levels, the synapse continues to code optimally by converting from high pass to low pass to accommodate photon noise (Srinivasan et al., 1982; Laughlin et al., 1987; van Hateren, 1992b; Juusola et al., 1995a). The mechanisms responsible for optimally tuning the synapse have not been identified previously, but the FP reported here is a strong contender.

Concluding remarks

Our recordings from blowfly compound eye demonstrate a large extracellular potential around photoreceptor output synapses, and our experiments indicate that changes in this field potential are dominated by the activity of photoreceptors and interneurons in an electrically isolated compartment, the lamina cartridge. This configuration forms a feedback loop, which modifies presynaptic signals without feedback synapses. An electrical feedback mechanism is economical, does not introduce synaptic noise, and can rapidly integrate and apply a reliable signal across a large number of synaptic release sites. These properties make it advantageous to use electrical feedback at photoreceptor output synapses.

References

Autrum H-J, Zettler F, Järvilehto M (1970) Postsynaptic potentials from a single monopolar neuron of the ganglion opticum I of the blowfly *Calliphora*. J Comp Physiol A Neuroethol Sens Neural Behav Physiol 70:414–424.

Barnes S (1994) After transduction: response shaping and control of transmission by ion channels of the photoreceptor inner segment. Neuroscience 58:447–459.

Bendat JS, Piersol AG (1971) Random data: analysis and measurement procedures. New York: Wiley Interscience.

Byzov AL, Shura-Bura TM (1986) Electrical feedback mechanisms in the processing of signals in the outer plexiform layers in the retina. Vis Res 26:33–44.

Byzov AL, Trifonov JA (1968) Response to electric stimulation of horizontal cells in the carp retina. Vis Res 8:817–822.

Chesler M, Kaila K (1992) Modulation of pH by neuronal activity. Trends Neurosci 15:396–402.

Faber DS, Korn H (1983) Field effects trigger post-anodal rebound excitation in vertebrate CNS. Nature 305:802–804.

Finkel AS, Redman S (1984) Theory and operation of a single microelectrode voltage clamp. J Neurosci Methods 11:101–127.

Fröhlich A, Meinertzhagen IA (1983) Quantitative features of synapse formation in the fly's visual system. I. The presynaptic photoreceptor terminal. J Neurosci 3:2336–2349.

Hardie RC (1987) Is histamine a neurotransmitter in insect photoreceptors? J Comp Physiol A 161:201–213.

Hardie RC (1989) A histamine-gated chloride channel involved in neurotransmission at a photoreceptor synapse. Nature 339:704–706.

Hardie RC, Weckström M (1990) Three classes of potassium channels in large monopolar cells of the blowfly *Calliphora vicina*. J Comp Physiol A Neuroethol Sens Neural Behav Physiol 167:723–736.

Harris FJ (1978) On the use of the windows for harmonic analysis with the discrete Fourier transform. Proc IEEE 66:51–83.

Järvilehto M, Zettler F (1971) Localized intracellular potentials from pre- and postsynaptic components in the external plexiform layer of an insect retina. J Comp Physiol A Neuroethol Sens Neural Behav Physiol 75:422–440.

Jefferys JG (1995) Nonsynaptic modulation of neuronal activity in the brain: electric currents and extracellular ions. Physiol Rev 75:689–723.

Juusola M, Kouvalainen E, Järvilehto M, Weckström M (1994) Contrast gain, signal-to-noise ratio and linearity in light-adapted blowfly photoreceptors. J Gen Physiol 104:593–621.

Juusola M, Uusitalo RO, Weckström M (1995a) Transfer of graded potentials at the photoreceptor interneuron synapse. J Gen Physiol 105:117–148.

Juusola M, Weckström M, Uusitalo RO, Korenberg MJ, French AS (1995b) Nonlinear models of the first synapse in the light-adapted fly retina. J Neurophysiol 74:2538–2547.

Juusola M, French AS, Uusitalo RO, Weckström M (1996) Information processing by graded-potential transmission through tonically active synapses. Trends Neurosci 19:292–297.

Kamermans M, Kraaij D, Spekreijse H (2001) The dynamic characteristics of the feedback signal from horizontal cells to cones in the goldfish retina. J Physiol 534:489–500.

Kirschfeld K (1967) Die Projektion der optischen umwelt auf das raster der rhabdomeren im komplexauge von musca. Exp Brain Res 3:248–270.

Kouvalainen E, Weckström M, Juusola M (1994) Determining photoreceptor signal-to-noise ratio in the time and frequency domains with a pseudorandom stimulus. Vis Neurosci 11:1221–1225.

Laughlin SB (1974) Neural integration in the first optic neuropile of dragonflies. II. Receptor signal interactions in the lamina. J Comp Physiol A Neuroethol Sens Neural Behav Physiol 92:357–375.

Laughlin SB (1981) Neural principles in the visual system. In: Handbook of sensory physiology, Vol VII/6B (Autrum H, ed), pp 133–280. Berlin-Heidelberg-New York: Springer.

Laughlin SB (1994) Matching coding, circuits, cells, and molecules to signals—general-principles of retinal design in the flys eye. Prog Retin Eye Res 13:165–196.

Laughlin SB, Hardie RC (1978) Common strategies for light adaptation in the peripheral visual systems of fly and dragonfly. J Comp Physiol A Neuroethol Sens Neural Behav Physiol 128:319–340.

Laughlin SB, Osorio D (1989) Mechanisms for neural signal enhancement in the blowfly compound eye. J Exp Biol 144:113–146.

Laughlin SB, Howard J, Blakeslee B (1987) Synaptic limitations to contrast coding in the retina of the blowfly Calliphora. Proc R Soc Lond B Biol Sci 231:437–467.

Lillywhite PG (1977) Single photon signals and transduction in an insect eye. J Comp Physiol A Neuroethol Sens Neural Behav Physiol 122:189–200.

Mote MI (1970) Focal recordings of responses evoked by light in the lamina ganglionaris of the fly Sarcophaga bullata. J Exp Zool 175:149–157.

Shaw SR (1975) Retinal resistance barriers and electrical lateral inhibition. Nature 255:480–482.

Shaw SR (1978) The extracellular space and blood-eye barrier in an insect retina: an ultrastructural study. Cell Tissue Res 188:35–61.

Shaw SR (1981) Anatomy and physiology of identified nonspiking cells in the photoreceptor-lamina complex of the compound eye of insects, especially Diptera. In: Neurons without impulses (Roberts A, Bush BMH, eds), pp 61–116. Cambridge, UK: Cambridge UP.

Shaw SR (1984) Early visual processing in insects. J Exp Biol 112:225–251.

Skingsley DR, Laughlin SB, Hardie RC (1995) Properties of histamine-activated chloride channels in the large monopolar cells of the dipteran compound eye: a comparative study. J Comp Physiol A Neuroethol Sens Neural Behav Physiol 176:611–623.

Srinivasan MV, Laughlin SB, Dubs A (1982) Predictive coding: a fresh view of inhibition in the retina. Proc R Soc Lond B Biol Sci 216:427–459.

Uusitalo RO, Weckström M (1994) The regulation of chloride homeostasis in the small nonspiking visual interneurons of the fly compound eye. J Neurophysiol 71:1381–1389.

Uusitalo RO, Juusola M, Kouvalainen E, Weckström M (1995a) Tonic transmitter release in a graded potential synapse. J Neurophysiol 74:470–473.

Uusitalo RO, Juusola M, Weckström M (1995b) Graded responses and spiking properties of identified first-order visual interneurons of the fly compound eye. J Neurophysiol 73:1782–1792.

van Hateren JH (1986) Electrical coupling of neuro-ommatidial photoreceptor cells in the blowfly. J Comp Physiol A Neuroethol Sens Neural Behav Physiol 158:795–811.

van Hateren JH (1992a) A theory of maximizing sensory information. Biol Cybern 68:23–29.

van Hateren JH (1992b) Theoretical predictions of spatiotemporal receptive fields of fly LMCs, and experimental validation. J Comp Physiol A Neuroethol Sens Neural Behav Physiol 171:157–170.

VanLeeuwen M, Fahrenfort I, Sjoerdsma T, Numan R, Kamermans M (2009) Lateral gain control in the outer retina leads to potentiation of center responses of retinal neurons. J Neurosci 29:6358–6366.

Weckström M, Kouvalainen E, Djupsund K, Järvilehto M (1989) More than one type of conductance is activated during responses of blowfly monopolar neurones. J Exp Biol 144:147–154.

Weckström M, Hardie RC, Laughlin SB (1991) Voltage-activated potassium channels in blowfly photoreceptors and their role in light adaptation. J Physiol 440:635–657.

Weckström M, Juusola M, Laughlin SB (1992a) Presynaptic enhancement of signal transients in photoreceptor terminals in the compound eye. Proc R Soc Lond B Biol Sci 250:83–89.

Weckström M, Kouvalainen E, Juusola M (1992b) Measurement of cell impedance in frequency domain using discontinuous current clamp and white noise modulated current injection. Pflügers Arch 421:469–472.

Zettler F, Järvilehto M (1971) Decrement-free conduction of graded potentials along the axon of a monopolar neuron. J Comp Physiol A Neuroethol Sens Neural Behav Physiol 75:402–421.

Zettler F, Straka H (1987) Synaptic chloride channels generating hyperpolarizing responses in monopolar neurones of the blowfly visual system. J Exp Biol 131:435–438.

Zheng L, de Polavieja GG, Wolfram V, Asyali MH, Hardie RC, Juusola M (2006) Feedback network controls photoreceptor output at the layer of first visual synapses in *Drosophila.* J Gen Physiol 127:495–510.

Zimmerman RP (1978) Field potential analysis and the physiology of second-order neurons in the visual system of the fly. J Comp Physiol 126:297–316.